Version of Record: https://www.sciencedirect.com/science/article/pii/S0306261919301278
Manuscript_176a7023626d61032963b2a43c381733

Ground sculpting to enhance energy yield of vertical bifacial solar farms

M. Ryyan Khan[1], Enas Sakr[2], Xingshu Sun[2], Peter Bermel[2], and Muhammad A. Alam[2, a)]
[1]*Department of Electrical and Electronic Engineering, East West University, Dhaka, Bangladesh*
[2]*Electrical and Computer Engineering Department, Purdue University, West Lafayette, IN 47907, USA*

The prospect of additional energy yield and improved reliability have increased commercial interest in bifacial solar modules. Recent publications have quantified the bifacial gain for several configurations. For example, a *standalone*, optimally-tilted bifacial panel placed over a *flat ground* (with 50% albedo) is expected to produce a bifacial energy gain of 30% (per module area). In contrast, self and mutual shading in a farm with periodically spaced panels reduces the bifacial gain to 10-15% (per farm area). Bifacial gain is negligible for vertical arrays — although the configuration is of significant interest since it can prevent soiling. Here, we calculate the bifacial gain of a solar farm where vertical arrays are placed over sculpted/patterned ground. We conclude that vertical panels straddling (upward) triangle-shaped ground maximizes the energy output. Also, based on a calculation of location-specific worldwide energy-yield map, the output gain of the optimum vertical panels with up-triangle ground configuration (with 50% albedo) compared to a traditional tilted monofacial design, i.e., the bifacial gain is (i) small up to 20° latitude, (ii) increases to 50% at 40° latitude, and (iii) reaches up to 100% at 60° latitude. Overall, high bifacial gains are observed in many regions particularly those with moderate to low clearness index. The enhanced output, along with reduced soiling loss and lower cleaning cost of the ground sculpted vertical bifacial (GvBF) solar farm could be of significant technological interest, especially in regions such as the Middle East and North Africa (MENA) susceptible to significant soiling losses.

1. Introduction and background

Monofacial panels are the most commonly used panel configuration in today's photovoltaic (PV) industry. Recent trends, however, show a steady increase in the share of bifacial panels in the PV market, and ITRPV also predicts further increases in the market share of bifacial PV over the next decade [1]. This prediction is not universally accepted since bifacial PV is typically more expensive. Unless bifacial power gains can offset any additional module costs, the technology would have a higher levelized cost of energy (LCOE).

Allowing light to be captured from both faces to create a 'bifacial' panel dates back to the early 1980s [2]–[4]. Luque et al. [2] demonstrated one of the earliest bifacial solar cells with n^+-p-n^+ transistor-like structure. Later, the same group predicted 50% [3] and 59% [4] gain using bifacial cells for two separate panel configurations. For example, Cuevas *et al.* [3] showed ~50% gain in bifacial output is possible, compared to a monofacial panel. However, this analysis requires painting the ground white and strategically placing white wall nearby to obtain such high gains. A more recent detailed numerical analysis by Sun *et al.* [5] predicts that the optimally placed bifacial panel over a flat ground will have energy gain of only 10% for an albedo of 25% (e.g., concrete). For artificially-treated ground with albedo 50% (e.g., white concrete), the bifacial gains can be 30%. These results agree with various independent calculations published in recent years [6]–[9]. Specifically, vertical standalone panels yield more energy than monofacial panels anywhere on earth for albedos above 0.35 [9]. For optimally tilted bifacial panels, up to a 25% bifacial gain is reported for panels in Cairo and Oslo (albedo 0.5) [6], a 30% gain is observed in Amsterdam (albedo 0.5) [7], and a ~30% gain in New Mexico for panels over high albedo (white boards) [8]. The bifacial gain, therefore, may not be as high as anticipated in the earliest studies.

The analysis of large solar farms consisting of periodic arrays of bifacial panels is even more complex due to mutual shading among the panels [10]–[13], as well as periodic ground shadowing [14], [15]. For instance, our recent work [15] showed that, for optimally designed farms, the vertical bifacial solar farm produces 10-30% *less* energy compared to an optimum monofacial farm. Although tilting the bifacial module does improve the yield [14], the attractive soiling-resistant property of vertical farm is lost. It has been shown numerically [16] as well as experimentally [17] that highly tilted panels are expected to accumulate dust at lower rates. Lower soiling translates into longer cleaning cycles, better-integrated energy yield, and lower cleaning costs.

Given the relatively small bifacial gain for vertical farms, one might consider resurrecting the ideas of Cuevas *et al.* (in the context of the solar farms) to improve the energy output of the bifacial solar farms. Recall that Cuevas *et al.* [3] obtained high bifacial gains by increasing the backside reflection from a white vertical wall. This configuration may be viewed as a cleverly-designed low-concentration bifacial PV. Indeed, there have been several designs and studies focusing on low-concentration for conventional PV [18]–[20] and bifacial PV systems [21]–[23]. Reflectors and concentrator structures between horizontal bifacial modules have been proposed and experimentally tested [24]. A concentrating photovoltaic-

a) Electronic mail: alam@purdue.edu.

thermal system using compound parabolic concentrator and a vertical bifacial panel has been shown to provide enhanced electrical and thermal energy output [25]. A recent study [23] experimentally demonstrated a comparison between flat and parabolic reflectors for tilted bifacial panels. We can now adapt these ideas for ground sculpting to vertical bifacial farms.

In this paper, we combine the idea of low concentration PV with vertical bifacial PV by artificially sculpting the ground to enhance albedo collection on the two faces of the panel. We have developed a model to analyze arbitrarily shaped ground between periodic arrays of vertical panels. The diurnal and seasonal variations of sun path and solar illumination are accounted for using our previously developed model [15]. Our analysis predicts that, among various configurations, ground mounted vertical bifacial panels with upward triangular ground shapes maximizes annual energy yield. For an effective albedo reflectance of $R_A \sim 50\%$, we observe that the designed bifacial PV farm in most cases yields more than a monofacial farm. In fact, at locations with low clearness index (higher diffuse light), the bifacial gain is higher; for example, at latitudes of 40° and 60°, the gains are ~50% and ~100% respectively. While $R_A \sim 50\%$ can be seen for white concrete, artificially designed white roofing foils can have $R_A > 80\%$ [26]. As discussed earlier, the reduced cleaning cost of the typical vertical bifacial solar farm (vBF) on flat ground may be offset by the subpar annual yield. On the other hand, our proposed ground sculpted vertical bifacial solar farm (GvBF) will yield more energy than the monofacial farm, in addition to the reduced cleaning cost. One must balance the additional gain of energy with the additional cost of ground-sculpting to assess its viability.

2. Numerical model.

In our numerical model (see Fig. 2 for a summary), we obtain the irradiance values from a NASA meteorological database [27]. The irradiance data and the panel array configuration are then used to find the light incident on the panel faces and the ground. Light scattered from the ground is partially collected by the bifacial panels. An electrical model for the panel then calculates the energy output corresponding to the collected sunlight. The hourly output is integrated to predict the annual yield. The calculation involves a non-trivial generalization of the view-factor method that have been used for flat-ground solar farm energy-yield calculations. Each calculation step is discussed in further details below.

2.1. Solar Data:

The daily average meteorological NASA data [27] is combined with the clear-sky model from Sandia [28] to calculate minute-by-minute variation of Global Horizontal Irradiance (GHI or I_{GHI}), Direct Normal Irradiance (DNI or I_b), Diffused Horizontal Irradiance (DHI or I_{diff}), solar azimuth angle γ_S, and solar zenith angle θ_Z, for any location in the world. The decomposition of GHI into DNI and DHI is based on Orgill and Hollands model [29], which is closely comparable to several other empirical models available in the literature [30]. Further details are provided in our prior publications [5], [15]. The use of NASA meteorological data ensures a statistically average estimate of GHI. This data can be readily be replaced by weather station data or predictive model GHI data [31], and our rest of the PV-farm model (discussed below) will calculate the corresponding solar farm output.

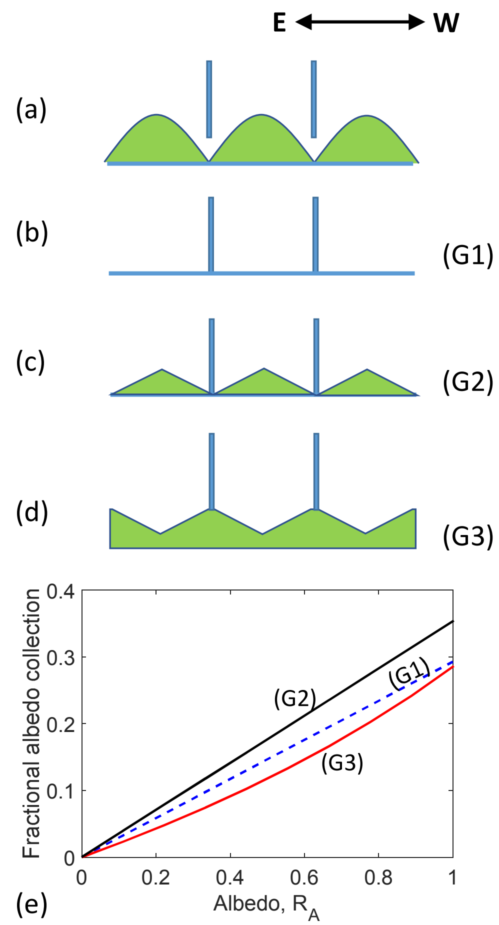

Fig. 1: East-West facing vertical bifacial panel array are shown. (a) shows the general configuration with vertical panel array elevated above arbitrarily shaped periodic ground pattern. (b)-(d) shows the flat ground (G1), upward triangle (G2), and downward triangle (G3) shaped ground between the vertical panels, respectively. (e) Collection of albedo as a fraction of normally incident direct light is compared for the different ground shapes.

2.2. Panels and array configuration:

In this paper, we consider an array of vertically placed bifacial panels facing East-West (E-W). Conventionally, the ground is kept horizontal and flat, as shown in Fig. 1 (b). However, intuitively, we expect additional albedo reflection if the ground is sculpted. In general, the panels may be elevated over arbitrarily patterned ground (as shown in Fig. 1 (a)). Since the vertical panel array is periodic, the ground pattern should be periodic (and symmetric) as well. For example, Fig. 1(b)-(d) shows the flat ground, upward triangle, and downward triangle shaped ground patterns between rows of panels. As we will see later, ground-mounted (i.e., zero elevation) panels on upward triangle-shaped ground pattern G2 in Fig. 1 (c) is close to the optimal configuration.

In early mornings and late afternoons, shadows cast by the sun are longer, which can create mutual shading between neighboring rows. Such non-uniform illumination may cause a reverse breakdown in series-connected cells. We assume three bypass diodes sub-dividing the panel to minimize the adverse effect of non-uniform illumination [32], and find the relevant output at the maximum power point. We do not include the effect of maximum power point trackers and inverters [33] on the farm output for this study.

2.3. Direct and diffused insolation collection (view factor method):

As the panels are E-W facing, it is straightforward to calculate the angle of incidence (AOI: $\theta^{(F)}$ or $\theta^{(B)}$) between the direct solar beam and the front (or back) face of the panel [15]. Assume that the panels are fixed at an elevation y_0 from the ground and arranged in an array as shown in Fig. 3(a). If the reflection, efficiency under normally incident direct light, and efficiency under diffused light for front $[R(\theta^{(F)}), \eta^{(F)}, \eta^{(F)}_{\text{diff}}]$ and back surfaces are all known, we can find the power generated per panel area at height z as follows [15]:

$$\hat{I}^{(F)}_{PV(dir)}(z) = [1 - R(\theta^{(F)})]\eta^{(F)} I_b \cos\theta^{(F)}, z > \text{shadow} \tag{1}$$

$$\hat{I}^{(F)}_{PV(diff)}(z) = \eta^{(F)}_{\text{diff}} [I_{\text{diff}} \times F_{dz-sky}] \tag{2}$$

Here, F_{dz-sky} is the view factor from a point z on the panel to the unobstructed sky. The power contribution from direct and diffused sunlight does not depend on the panel-to-ground distance, nor the shape or reflectivity of the ground (assuming it does not cast shadows on the panels).

In general, a view factor F_{A-B} represents the fraction of radiation collected by surface B emitted from surface A. The expressions for the view factors used in this paper are straightforward and can be found in prior literature [15], [34] or textbooks [35].

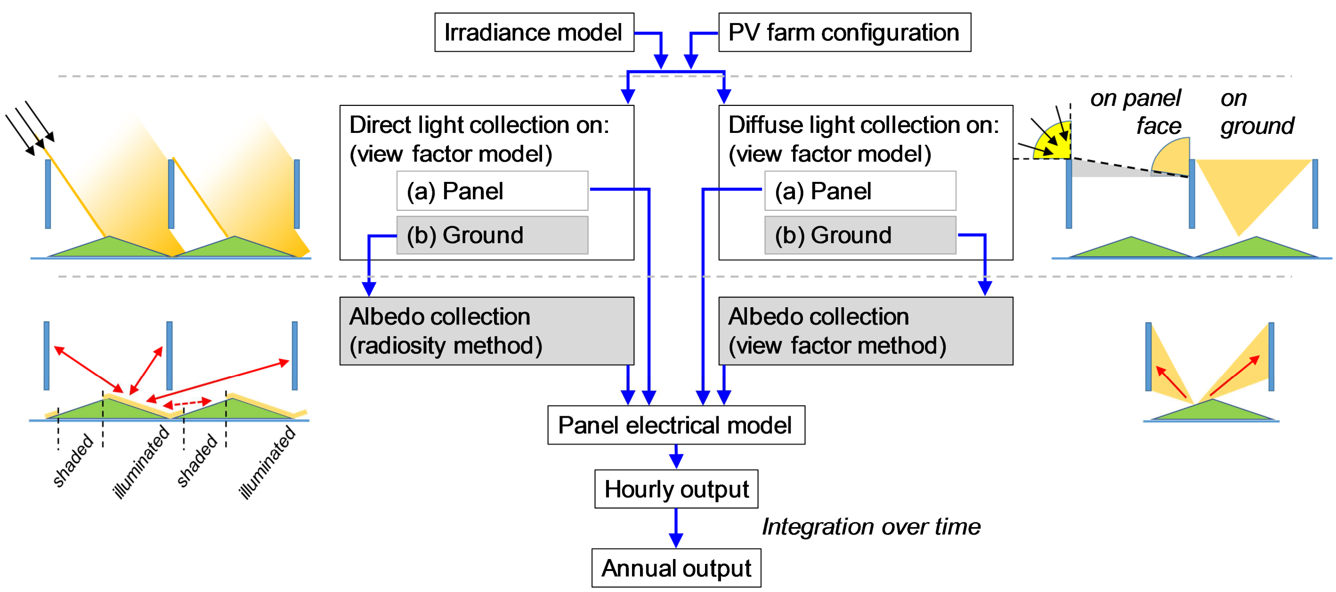

Fig. 2: Calculation flow for determining the output of ground sculpted vertical bifacial PV (GvBF) farm.

2.4. Albedo from diffused sunlight (view factor method):

To calculate the collection of diffuse sunlight via albedo reflection, we first find the amount of diffuse sunlight collected on the sculpted ground under the PV array. Then we can assume the light reflected by the ground serves as a source for the panels to collect. The amount of diffuse illumination hitting segment Δs on the sculpted ground can be written as:

$$I_{\text{Gnd:diff}}(s) = I_{\text{diff}} \times F_{\Delta s-\text{sky}}(s) \tag{3}$$

Here, $F_{\Delta s-\text{sky}}(s)$ is the view factor from the segment Δs at position s on the ground to the unobstructed part of the sky. We can now write the corresponding albedo collection on the panels (front face) as follows:

$$\hat{I}^{(F)}_{PV(Alb:diff)}(z) = \eta^{(F)}_{\text{diff}} \sum_{s} \left[R_A \, I_{\text{Gnd:diff}}(s) \Delta s \, F^{(F)}_{dz-\Delta s} \right] \tag{4}$$

Here, $F^{(F)}_{dz-\Delta s}$ is the view factor from position z on the panel to the ground segment. The contribution from adjacent periods in the array is small; we therefore only consider the collection of light from ground to panels within the relevant period.

2.5. Albedo from direct sunlight (radiosity method):

The configuration shown in Fig. 3(a) can, in general,ct have any arbitrarily sculpted ground—however, we restrict our analysis to cases when the sculpted ground does not cast any additional shadow on panels. Diffuse ground reflection can be accounted for using view factor analysis. However, in the presence of multiple diffuse surfaces, multiple reflections can occur, which can be accounted for using ray tracing [35]. The radiosity method is used to trace diffuse reflections from multiple surfaces in an enclosure. This technique has its basis in computing heat transfer between diffuse surfaces in an enclosure [35] as well as rendering images in computer graphics [36]. Here, we provide a brief summary of the method. The radiosity is defined as the total energy leaving a surface area with diffuse reflection property. In an enclosure, the radiosity b_i of an element of index i is computed using the following equation:

$$b_i = \sum_j \rho_j b_j F_{ji} + e_i, \tag{5}$$

where ρ_j is the diffuse reflection of each element. In Eq. (5), the initial reflection from an element of index i is $e_i = \rho_i H_i$, where H_i is the initial solar irradiation received on the ground element. The view factor between surface elements F_{ji} accounts for multiple reflections between surfaces enclosed.

In an enclosure with N surface elements, eq. (5) can be translated into the matrix equation

$$B = (\boldsymbol{I} - \rho \boldsymbol{F})^{-1} E, \tag{6}$$

where $B^T = [b_1 \, b_2 \, \cdots \, b_N]$, $E^T = [e_1 \, e_2 \, \cdots \, e_N]$. The view factor matrix $\boldsymbol{F}$ contains the mutual view factors between elements involved in the enclosure, with self-view factors $F_{ii} = 0$, since all elements are assumed to be locally flat.

It is worth mentioning that the radiosity computation in its form in eq. (6) is computationally expensive in general. However, for the problem in hand, with a few surfaces involved, each can be decomposed into a finite number of elements. The accuracy of the solution is well-maintained with a minimal number of segments, without the need to use the progressive refinement approach [37].

For the problem of an array of periodic vertical solar panels mounted on or elevated above the ground, we assume that the ground and the panels are infinitely extended in one direction. Thus, the corresponding view factors can be simply computed using the crossed-strings method [35]. A single panel is assigned a single index and zero reflectivity while the ground is decomposed into a number of segments having an albedo reflectivity R. Hence, the normalized fractional power received on a single panel due to direct albedo reflection is the first element of the vector $P = \boldsymbol{F}B$. The calculation is performed for both the front and back surfaces of the panel. Hence, the power generated by reflected direct sunlight can be written as:

$$\hat{I}^{(F)}_{PV(Alb:dir)}(z) = \eta^{(F)}_{\text{diff}} \left[I_{\text{dir}} \times P(1) \right]. \tag{7}$$

In principle, elevated panels above the ground surface can receive albedo light reflection from all exposed points on the ground. However, the view factors between a given panel and a ground segment will decrease considerably with separation [38]. Hence, a good first order approximation is to consider two periods of the full array. This arrangement is depicted in the bottom left of Fig. 2.

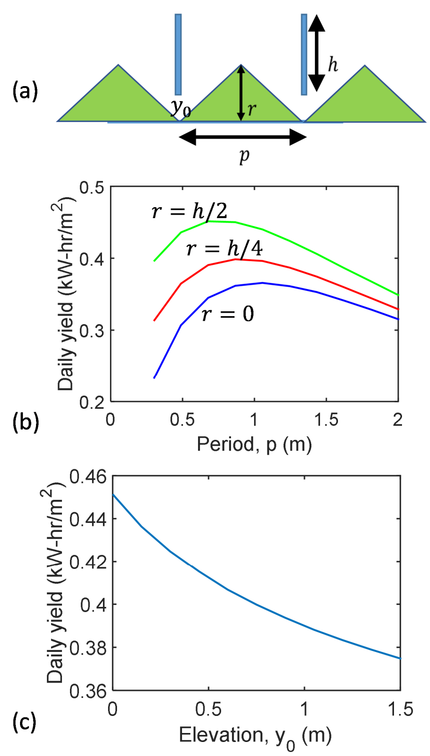

Fig. 3: (a) Vertical bifacial panel array placed elevated y_0 from an upward triangular ground. (b) Daily yield (per land area) of the solar farm (with $y_0 = 0$) as a function of ground triangle height r and array period p. (c) Daily yield (per land area) is shown as a function of the panel elevation y_0. The values of r and period p are co-optimized at each y_0. The calculations are for Washington DC (Sept. 22).

The shadow of the panel on the ground changes with the solar elevation angle. Over the course of the day, only ground regions exposed to sunlight provide direct albedo reflection. In some situations, an adjacent panel or a sculpted ground segment can partially block the light reflected by the ground, thus reducing the view factor between ground segments and the panel. These situations are all computed carefully in the model.

Similar calculations will result in the illumination collection components for the back face as well. All the light collection components by the panel faces are now used to estimate hourly panel output (assuming 3 bypass diodes per panel) based on the analytical approach in Ref. [32]. Instead of individual panel output, we focus on the farm yield (i.e., output per land area). The diurnal results are integrated to obtain monthly and annual farm yield.

The model described above can calculate the albedo light collection from an arbitrarily curved surface. The curved surface is symmetric around the center of the period due to the vertical panel array configuration. Therefore, as a first-order estimate, using Hottel's crossed string rule [35], we see that the curved surface can be replaced by two straight lines. For example, a periodic upward hemispherical ground pattern would be equivalent to the upward triangular ground pattern. That is why, for the rest of the paper, we will focus on triangular ground shapes shown in Fig. 1 (c, d).

3. Optimization of a ground-sculpted solar farm.

Here, we wish to answer three questions: (i) Is there an optimum ground pattern? (ii) Given the pattern, what is the optimum period for the panel array? (iii) What improvement, if any, can we expect from the optimized panel array?

Consider the three ground patterns shown in Fig. 1(b)-(d): the flat ground, upward triangle, and downward triangle, labeled G1, G2, and G3, respectively. When the sun is exactly normal to the ground (e.g., noon at the equator), there is no shading on the ground from the direct light. In such a scenario, the albedo light collection as a fraction of the direct light is shown for various albedos R_A. As expected, for the flat ground G1 shown in Fig. 1(b), the fractional albedo collection increases linearly with R_A. At $R_A = 1$, the light collection is limited by both the view factor from the ground to the sky, and the view factor from the panel face to the ground. For the downward triangle G3 in Fig. 1 (d), the fractional albedo collection is worse than G1 in Fig. 1 (b) for $R_A < 1$. This is because some light bounces between the mutually inclined ground regions, which incurs loss from each bounce if $R_A < 1$. Finally, the upward triangle G2 shown in Fig. 1 (c) is shaped to reflect the light primarily towards the panel faces, and as seen in Fig. 1(e), G2 shows $> 15\%$ increase in fractional albedo collection compared to the trivial flat ground G1.

Now that we know we want to choose the up-triangle ground shape for better output, we need to optimize the 'ground sculpted vertical bifacial PV farm' design. Given a specific panel size (width $h = 1$ m), the parameters that define this PV farm are: period of panel array p, panel elevation from ground y_0, and the height of the ground triangle r as shown in Fig. 3(a).

Fig. 3(b) shows the integrated output of a given day (Sep. 22) in Washington DC for $y_0 = 0$. The line marked $r = 0$ corresponds to the conventional flat ground consistent with our prior work [15]. The daily yield per land area has an optimum period p. For small p, mutual shading quickly degrades the output. And, at larger p, the panels miss a large fraction of light hitting the ground.

Next, as we increase the height r of the triangular ground, essentially tilting the ground towards the panel, thereby steering the albedo light mostly towards the panel faces. As a result, we observe that the output increases as we increase r. However, if r is increased beyond $h/2$, the ground would cast a shadow on the panels, reducing the output dramatically. Therefore, for ground-mounted panels (i.e., $y_0 = 0$), the triangular ground height can at most be half the panel size, i.e., $r = h/2$—and, as discussed above, this will also result in the highest possible output with optimized period p. In general, we would choose $r = y_0 + h/2$ for panels fixed at elevation y_0.

Finally, we need to optimize y_0. As we increase y_0, the 'viewing angle', i.e., view factor between a panel face and the illuminated part of the ground reduces, thereby reducing the albedo collection. Moreover, with increasing y_0, larger regions of the ground are exposed to each other. This increases light scattering in between the ground faces [similar to the ground shape G3 in Fig. 1 (d)] and increases scattering loss on the ground. We conclude that ground mounting ($y_0 = 0$) the panels are the best choice for this configuration. On the other hand, as seen in the literature [6], [5], the standalone tilted bifacial panels collect more albedo light with increased y_0. The monotonic decrease in output with y_0 is specific to vertical bifacial panel array. Our explanation is also supported by a detailed numerical analysis shown in Fig. 3(c), indicating a monotonous decrease in daily yield as y_0 is increased. In this plot (p, r)-pair is optimally chosen for each value of y_0.

To summarize, we can set $y_0 = 0$, $r = h/2$ and then optimize period p to maximize yearly yield. The optimum value of p will depend on the location on earth and the weather (i.e., clearness index).

4. Energy yield at a specific latitude.

Let us now focus specifically on various locations on earth at latitude 40°N. At a given latitude, sunlight travels through the same thickness of atmosphere (air mass). This results in the same terrestrial insolation under a clear sky assumption. However, as the sky clearness is different at various longitudes, we observe variation in GHI, DNI, and DHI, even at the same latitude. We compare the yearly yield of ground sculpted vertical bifacial PV farm (GvBF, Fig. 1 (c)), conventional vertical bifacial PV farm (vBF, Fig. 1 (b)), and optimally tilted south-facing monofacial PV farm in Fig. 4. We assume an extra 10% loss in output due to soiling for the tilted monofacial panels; in practice, the soiling loss can be considerably higher [39], [40]. For example, a study in Egypt has shown a horizontal surface to have 4-5 times higher soiling rate compared to a vertical surface [17].

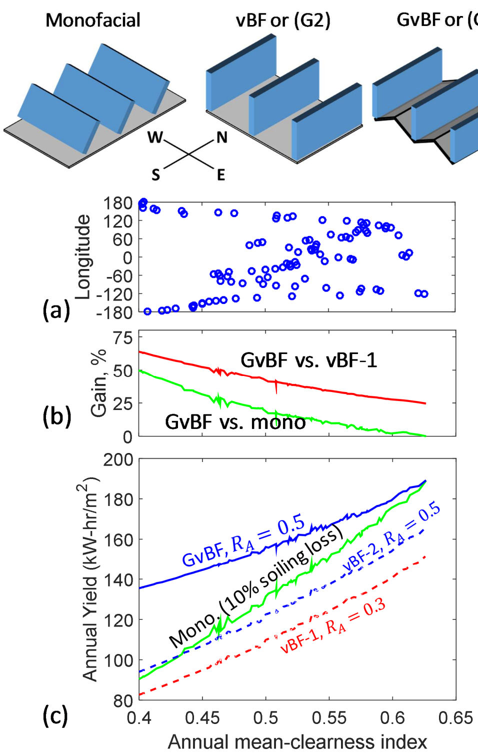

Fig. 4: The annual energy yield of various monofacial and bifacial PV farm configurations as a function of clearness index (at latitude 40°N) are shown in (c). The vBF solar farms with flat ground and $R_A = 0.3$ and 0.5 are indicated as vBF-1 and vBF-2, respectively. The output gain observed in GvBF compared to other configurations are shown in (b). (a) shows the longitude locations corresponding to the clearness index values at latitude 40°N.

The integrated annual yields of the various PV farms (optimized) are shown in Fig. 4(c). In all cases, output increases with annual mean clearness index k_{TA} as the input GHI is high at higher k_{TA}. For monofacial PV, we assume 10% output penalty due to higher soiling compared to vertical panels. There is a 15% or more loss in output of vBF with typical ground albedo reflection $R_A = 0.3$ (the earth's average albedo) compared to the monofacial PV farm. Even if the albedo is increased to $R_A = 0.5$ by covering the ground with artificial material, the vBF cannot exceed or match the monofacial farm.

The GvBF (with $R_A = 0.5$) shows an exceptional advantage over vBF as well as monofacial farm. As shown in Fig. 4(b), the GvBF shows up to 50% gain in output compared to monofacial farm, especially in cloudy regions (low k_{TA}). A closer observation of earth's map and Fig. 4(a) indicates that $k_{TA} > 0.6$ occurs primarily over oceans. Therefore, at all locations of interest (i.e., land), GvBF yields higher output than monofacial farms.

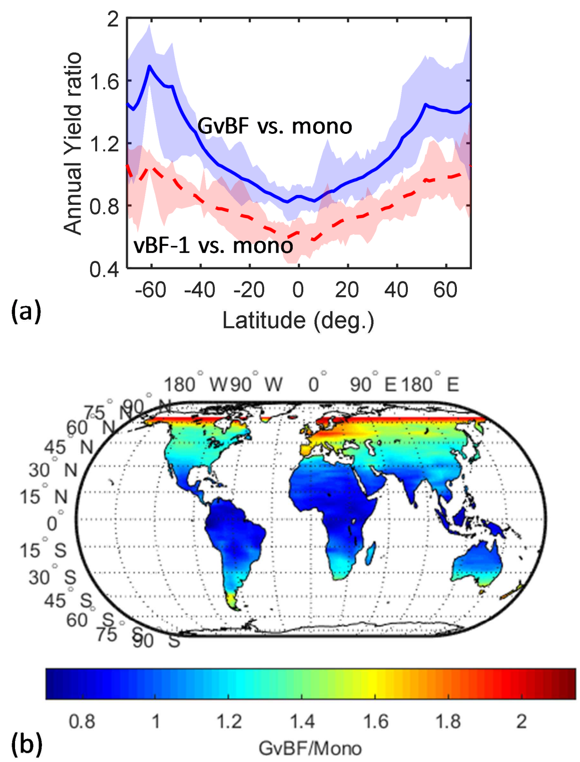

Fig. 5: Annual yield of vBF, GvBF, and monofacial solar farms are compared from a global perspective. (a) For various latitudes, ratio of annual yields of GvBF ($R_A = 0.5$) vs. monofacial farm, and of vBF-1 ($R_A = 0.3$) vs. monofacial farm are shown by solid and dashed lines respectively. The monofacial farm includes a 10% soiling loss. The shaded regions along with the lines represent the spread in data for various longitudes. (b) A worldwide annual yield ratio of GvBF vs monofacial solar farm is shown.

5. A World map of energy yield.

5.1. Energy yield and bifacial gain:

To analyze if the large improvement in GvBF output seen at a latitude of 40°N is common elsewhere, we perform a world-wide comparative study of vBF, GvBF, and monofacial farm (see Fig. 5). The vBF farm with flat ground and $R_A = 0.3$ (marked vBF-1) yields less than monofacial farm (10% soiling loss assumed) for most locations worldwide, as seen by the dashed line in Fig. 5(a). This is consistent with prior literature [15]. The GvBF farm output is much higher than the vBF farm, and comparable to or higher than the monofacial farm. The annual yield ratio between GvBF and monofacial farms is shown by the solid line in Fig. 5(a). The shaded plot represents the spread in data for various longitudes. From the solid line in Fig. 5(a), we observe that: (i) at lower latitudes ($< 20°$), GvBF output is comparable to that of a monofacial farm, (ii) for latitudes beyond $20°$, the GvBF consistently yields more energy than the monofacial farm. In fact, once we analyze the shaded plot (i.e., output variations for different longitudes), we see that there are several locations even for latitudes $< 20°$ where the GvBF output is the highest.

Closer to the equator and for low latitudes, the sun-path is less tilted, the sunlight is predominantly direct, and the optimal tilt of the panels are close to horizontal. Given these facts, it is trivial to predict that monofacial should be the better choice for these locations. As we move to higher latitudes, the gain from GvBF consistently increases. At high latitudes ($\sim 60°$), the GvBF produces a factor of two higher energy (~100% gain) compared to the monofacial farm. Finally, a more detailed picture of GvBF to monofacial output ratio is shown in Fig. 5(b), which is a global map of the results from Fig. 5(a).

5.2. *Explaining the high bifacial gain:*

At higher latitudes, the sun stays lower in the sky, and the fraction of diffuse light typically increases. These two factors explain the improvement in bifacial gain as follows. For clarity, we will discuss the energy gains in the Northern hemisphere only; of course, similar considerations also apply to the Southern hemisphere.

First, the optimal tilt for the monofacial panels increases with latitude, to face the highly tilted path of the sun. As a result, longer shadows are cast to the North, especially in winter. The spacing among South-facing monofacial panels, therefore, must increase to minimize shading losses. Consequently, we lose sunlight on the ground in summer when the shadow is shorter. In contrast, long shadows to the North do not affect the East-West facing vertical farms discussed here. The difference in the shadowing loss is the first reason why vertical farms produce significantly more energy than the monofacial farms.

Second, a monofacial panel collects less diffuse light (on its single collection face) as it is tilted at a higher angle. In contrast, bifacial vertical panels remain equally effective in collecting diffuse light at any latitude. Therefore, as the fraction of diffuse light increases at higher latitudes, the collection of sunlight by monofacial panels decreases compared to bifacial panels. In fact, the interplay between the sun-path and the diffuse light on monofacial vs. vertical bifacial panels are complicated, but been discussed in detail in our prior work (see Section 3.4.1 in ref. [15]).

Note that the enhanced output of bifacial farms also requires closer packing of bifacial modules. Therefore, a cost-benefit analysis must carefully weigh the increased energy yield against the need for additional modules.

The ground pattern for the GvBF solar farm would be artificially sculpted, and the ground material may not necessarily be natural (grass or sand). Although we choose $R_A = 0.5$ for our artificial material, un-weathered white roofing membranes may have $R_A \sim 0.88$ [26]. With time, this reflectance would decrease; however, $R_A = 0.5$ could still be a conservative estimate with occasional maintenance [26].

5.3. *Sources of variability in the analysis:*

Finally, we realize that there will local variability around the average yield predicted so far during the practical implementation of the GvBF system. *First*, the NASA meteorological databased used for the studies in this paper is monthly insolation data averaged over 22 years. While this provides a statistically relevant result, a more detailed minute-by-minute insolation data will provide a location-specific accurate prediction. Recent calculations show that with rigorous angle-dependent DHI, the model on average differs from the field measurement only by a few percents (see Table 1 in [5]). *Second*, our view factor model does not consider angle-dependent diffuse light collection. Our primary estimates suggest that the final result based on the simpler isotropic model versus the angle-dependent model differs by only a few percent. Therefore, we anticipate a good agreement with the overall experimental results and the overall conclusions in the paper. As field results become available, a more rigorous modeling effort would be justified. *Third*, the optimal geometrical configuration of the PV array may have variations during installations. A closer study of the data in Fig. 3(b) shows that 10% variations in p and/or r results in less than 5% variation in output. *Fourth*, we have assumed uniform ground reflectance R_A. We also did not consider the spectral distribution of R_A. Spectral variations, however, lead to ~5% variation (e.g., for white sand) in the calculated energy output, as discussed in prior literature [41].

6. Summary and Conclusions.

In this work, we presented a numerical model for our proposed vertical bifacial panel array, elevated to a specified height upon intentionally patterned ground. In summary:

1. A vertical bifacial solar farm (vBF) is of interest due to its reduced soiling and cleaning costs. However, a typical vBF over flat ground severely underperforms compared to monofacial solar farms. Despite other advantages, the reduced energy yield is a major hurdle to flat-ground vBF adoption. Thus, we proposed a novel ground patterned vBF (GvBF) configuration to significantly enhance energy output. The optimum GvBF is simple enough for practical implementation, and the yield is predicted to surpass the conventionally tilted monofacial solar farms.
2. To analyze the proposed GvBF configuration, we extended

our prior vBF model in a non-trivial manner. Our new calculation method uses a combination of view-factor and radiosity methods to include the effects of direct and diffused sunlight, albedo, and the corresponding shadows for elevated panel array and ground patterning for the new solar farm configuration.

3. The model was applied to co-optimize panel spacing, elevation and ground shape for maximum annual yield. We found an optimum condition is achieved when vertical panels of size h are placed on the ground (no elevation) with the ground sculpted into an upward triangle pattern with height $h/2$.
4. Using a ground material with an effective albedo reflection $R_A = 0.5$, the optimal ground sculpted vertical bifacial PV farm (GvBF) yields more energy than the monofacial farm in most locations worldwide, particularly in cloudier regions. For example, at latitude 40°N, the bifacial gain of GvBF over the monofacial farm is 30-50% for cloudy regions (clearness index $k_{TA} < 0.45$) and diminishes for more clear-sky regions.
5. The optimized GvBF energy yield has been compared to the conventionally tilted monofacial solar farms for all locations worldwide. In fact, compared to the optimum monofacial farm, the GvBF has 50% and 100% more annual energy output at latitudes 40° and 60° respectively, in regions with somewhat cloudy skies ($k_{TA} < 0.45$).

Here, we have focused on vertical bifacial panel arrays, which can have much less soiling than tilted monofacial panels. In our analysis, we have assumed an extra 10% soiling loss for the tilted monofacial panels. This value is not absolute for all practical situations—it will vary with the local soiling rate as well as the cleaning cycle—and can be much worse. In the end, the integrated energy output along with bifacial versus monofacial panel costs, maintenance [42] and the cleaning costs [43] (integrated over the farm lifetime) will define the difference in the levelized cost of energy (LCOE) [44]. In our studies of energy yields, we found that the proposed GvBF configuration will have significant advantages over the conventional monofacial farms, especially, but not only, in moderately to highly-cloudy locations.

Acknowledgment

We gratefully acknowledge Dr. Chris Deline from NREL, and Dr. Joshua S. Stein and Dr. Cliff Hansen from Sandia National Laboratories for helpful discussions. This work was partly supported by the National Science Foundation under Grant No. #1724728, and the Solar Energy Research Institute for India and the U.S. (SERIIUS) funded jointly by the U.S. Department of Energy subcontract DE AC36-08G028308 and the Government of India subcontract IUSSTF/JCERDC-SERIIUS/2012. Support was also provided by the National Science Foundation Award EEC 1454315 – CAREER: Thermophotonics for Efficient Harvesting of Waste Heat as Electricity, the Department of Energy, under DOE Cooperative Agreement No. DE-EE0004946 (PVMI Bay Area PV Consortium), and the NCN-NEEDS program under Contract 1227020-EEC.

Supplementary material

The following tabulated data are provided as supplementary materials. These files include information for a monofacial farm (no soiling), a vertical bifacial farm (albedo 0.3), and a ground sculpted vertical bifacial farm. Each farm has its period optimized to maximize annual yield. The tilt of the monofacial panels are a function of latitude, see ref [45].

TableS1_Yield_data.xlsx : Annual yield of the solar farms per land area (kWh/m^2)

TableS2_arrayPeriod_data.xlsx : Optimum array period (normalized by the panel size h) of each of the farms.

References

[1] “International Technology Roadmap for Photovoltaic Results 2015, Seventh edition,” ITRPV, Oct. 2016.

[2] A. Luque, A. Cuevas, and J. M. Ruiz, “Double-sided n+-p-n+ solar cell for bifacial concentration,” *Sol. Cells*, vol. 2, no. 2, pp. 151–166, Oct. 1980.

[3] A. Cuevas, A. Luque, J. Eguren, and J. del Alamo, “50 Per cent more output power from an albedo-collecting flat panel using bifacial solar cells,” *Sol. Energy*, vol. 29, no. 5, pp. 419–420, 1982.

[4] A. Luque, E. Lorenzo, G. Sala, and S. López-Romero, “Diffusing reflectors for bifacial photovoltaic panels,” *Sol. Cells*, vol. 13, no. 3, pp. 277–292, Jan. 1985.

[5] X. Sun, M. R. Khan, C. Deline, and M. A. Alam, “Optimization and performance of bifacial solar modules: A global perspective,” *Appl. Energy*, vol. 212, pp. 1601–1610, Feb. 2018.

[6] U. A. Yusufoglu, T. M. Pletzer, L. J. Koduvelikulathu, C. Comparotto, R. Kopecek, and H. Kurz, “Analysis of the Annual Performance of Bifacial Modules and Optimization Methods,” *IEEE J. Photovolt.*, vol. 5, no. 1, pp. 320–328, Jan. 2015.

[7] G. J. M. Janssen, B. B. Van Aken, A. J. Carr, and A. A. Mewe, “Outdoor Performance of Bifacial Modules by Measurements and Modelling,” *Energy Procedia*, vol. 77, pp. 364–373, Aug. 2015.

[8] M. Lave, J. S. Stein, and L. Burnham, “Performance Results for the Prism Solar Installation at the New Mexico Regional Test Center: Field Data from February 15 - August 15, 2016,” Sandia National Laboratories., Albuquerque, NM, SAND2016-9253, 2016.

[9] S. Guo, T. M. Walsh, and M. Peters, “Vertically mounted bifacial photovoltaic modules: A global analysis,” *Energy*, vol. 61, pp. 447–454, Nov. 2013.

[10] D. Passias and B. Källbäck, “Shading effects in rows of solar cell panels,” *Sol. Cells*, vol. 11, no. 3, pp. 281–291, Apr. 1984.
[11] J. Bany and J. Appelbaum, “The effect of shading on the design of a field of solar collectors,” *Sol. Cells*, vol. 20, no. 3, pp. 201–228, Apr. 1987.
[12] N. Y. Fathi and A. Samer, “View Factors of Flat Solar Collectors Array in Flat, Inclined, and Step-Like Solar Fields,” *J. Sol. Energy Eng.*, vol. 138, no. 6, pp. 061005-061005–8, Sep. 2016.
[13] J. Appelbaum, “View Factors to Grounds of Photovoltaic Collectors,” *J. Sol. Energy Eng.*, vol. 138, no. 6, pp. 064501-064501–6, Sep. 2016.
[14] J. Appelbaum, “Bifacial photovoltaic panels field,” *Renew. Energy*, vol. 85, pp. 338–343, Jan. 2016.
[15] M. R. Khan, A. Hanna, X. Sun, and M. A. Alam, “Vertical bifacial solar farms: Physics, design, and global optimization,” *Appl. Energy*, vol. 206, no. Supplement C, pp. 240–248, Nov. 2017.
[16] H. Lu, L. Lu, and Y. Wang, “Numerical investigation of dust pollution on a solar photovoltaic (PV) system mounted on an isolated building,” *Appl. Energy*, vol. 180, pp. 27–36, Oct. 2016.
[17] H. K. Elminir, A. E. Ghitas, R. H. Hamid, F. El-Hussainy, M. M. Beheary, and K. M. Abdel-Moneim, “Effect of dust on the transparent cover of solar collectors,” *Energy Convers. Manag.*, vol. 47, no. 18, pp. 3192–3203, Nov. 2006.
[18] S. Nann, “Potentials for tracking photovoltaic systems and V-troughs in moderate climates,” *Sol. Energy*, vol. 45, no. 6, pp. 385–393, Jan. 1990.
[19] V. Poulek and M. Libra, “A new low-cost tracking ridge concentrator,” *Sol. Energy Mater. Sol. Cells*, vol. 61, no. 2, pp. 199–202, Mar. 2000.
[20] N. Sarmah and T. K. Mallick, “Design, fabrication and outdoor performance analysis of a low concentrating photovoltaic system,” *Sol. Energy*, vol. 112, pp. 361–372, Feb. 2015.
[21] A. W. Finkl, “Solar energy concentrator apparatus for bifacial photovoltaic cells,” US5538563 A, 23-Jul-1996.
[22] V. Poulek, A. Khudysh, and M. Libra, “Innovative low concentration PV systems with bifacial solar panels,” *Sol. Energy*, vol. 120, pp. 113–116, Oct. 2015.
[23] H. Nussbaumer *et al.*, “Influence of Low Concentration on the Energy Harvest of PV Systems Using Bifacial Modules,” WIP, 2016.
[24] Y. S. Lim, C. K. Lo, S. Y. Kee, H. T. Ewe, and A. R. Faidz, “Design and evaluation of passive concentrator and reflector systems for bifacial solar panel on a highly cloudy region – A case study in Malaysia,” *Renew. Energy*, vol. 63, pp. 415–425, Mar. 2014.
[25] D. Cabral and B. O. Karlsson, “Electrical and thermal performance evaluation of symmetric truncated C-PVT trough solar collectors with vertical bifacial receivers,” *Sol. Energy*, vol. 174, pp. 683–690, Nov. 2018.
[26] “Calculating the additional energy yield of bifacial solar modules,” SolarWorld, White paper, 2016.
[27] POWER, “Surface meteorology and Solar Energy: A renewable energy resource web site (release 6.0),” 2017. [Online]. Available: https://eosweb.larc.nasa.gov/cgi-bin/sse/sse.cgi? [Accessed: 06-Jan-2017].
[28] *PV Performance Modeling Collaborative | An Industry and National Laboratory collaborative to improve Photovoltaic Performance Modeling*. 2016.
[29] J. F. Orgill and K. G. T. Hollands, “Correlation equation for hourly diffuse radiation on a horizontal surface,” *Sol. Energy*, vol. 19, no. 4, pp. 357–359, Jan. 1977.
[30] L. T. Wong and W. K. Chow, “Solar radiation model,” *Appl. Energy*, vol. 69, no. 3, pp. 191–224, Jul. 2001.
[31] L. M. Halabi, S. Mekhilef, and M. Hossain, “Performance evaluation of hybrid adaptive neuro-fuzzy inference system models for predicting monthly global solar radiation,” *Appl. Energy*, vol. 213, pp. 247–261, Mar. 2018.
[32] C. Deline, A. Dobos, S. Janzou, J. Meydbray, and M. Donovan, “A simplified model of uniform shading in large photovoltaic arrays,” *Sol. Energy*, vol. 96, pp. 274–282, Oct. 2013.
[33] C. R. Sánchez Reinoso, D. H. Milone, and R. H. Buitrago, “Simulation of photovoltaic centrals with dynamic shading,” *Appl. Energy*, vol. 103, pp. 278–289, Mar. 2013.
[34] J. Appelbaum, “The role of view factors in solar photovoltaic fields,” *Renew. Sustain. Energy Rev.*, vol. 81, pp. 161–171, Jan. 2018.
[35] M. F. Modest, *Radiative heat transfer*, Third Edition. New York: Academic Press, 2013.
[36] C. M. Goral, K. E. Torrance, D. P. Greenberg, and B. Battaile, “Modeling the Interaction of Light Between Diffuse Surfaces,” *SIGGRAPH Comput Graph*, vol. 18, no. 3, pp. 213–222, Jan. 1984.
[37] M. F. Cohen, S. E. Chen, J. R. Wallace, and D. P. Greenberg, “A progressive refinement approach to fast radiosity image generation,” *ACM SIGGRAPH Comput. Graph.*, vol. 22, no. 4, pp. 75–84, 1988.
[38] J. Appelbaum, “Current mismatch in PV panels resulting from different locations of cells in the panel,” *Sol. Energy*, vol. 126, no. Supplement C, pp. 264–275, 2016.
[39] T. Sarver, A. Al-Qaraghuli, and L. L. Kazmerski, “A comprehensive review of the impact of dust on the use of solar energy: History, investigations, results, literature, and mitigation approaches,” *Renew. Sustain. Energy Rev.*, vol. 22, pp. 698–733, Jun. 2013.
[40] J. J. John, V. Rajasekar, S. Boppana, S. Chattopadhyay, A. Kottantharayil, and G. TamizhMani, “Quantification and Modeling of Spectral and Angular Losses of Naturally Soiled PV Modules,” *IEEE J. Photovolt.*, vol. 5, no. 6, pp. 1727–1734, Nov. 2015.
[41] T. C. R. Russell, R. Saive, A. Augusto, S. G. Bowden, and H. A. Atwater, “The Influence of Spectral Albedo on Bifacial Solar Cells: A Theoretical and Experimental Study,” *IEEE J. Photovolt.*, vol. 7, no. 6, pp. 1611–1618, Nov. 2017.

[42] L. Peters and R. Madlener, “Economic evaluation of maintenance strategies for ground-mounted solar photovoltaic plants,” *Appl. Energy*, vol. 199, pp. 264–280, Aug. 2017.
[43] S. You, Y. J. Lim, Y. Dai, and C.-H. Wang, “On the temporal modelling of solar photovoltaic soiling: Energy and economic impacts in seven cities,” *Appl. Energy*, vol. 228, pp. 1136–1146, Oct. 2018.
[44] C. S. Lai and M. D. McCulloch, “Levelized cost of electricity for solar photovoltaic and electrical energy storage,” *Appl. Energy*, vol. 190, pp. 191–203, Mar. 2017.
[45] A. Luque and S. Hegedus, Eds., *Handbook of Photovoltaic Science and Engineering, Second Edition*. 2011.

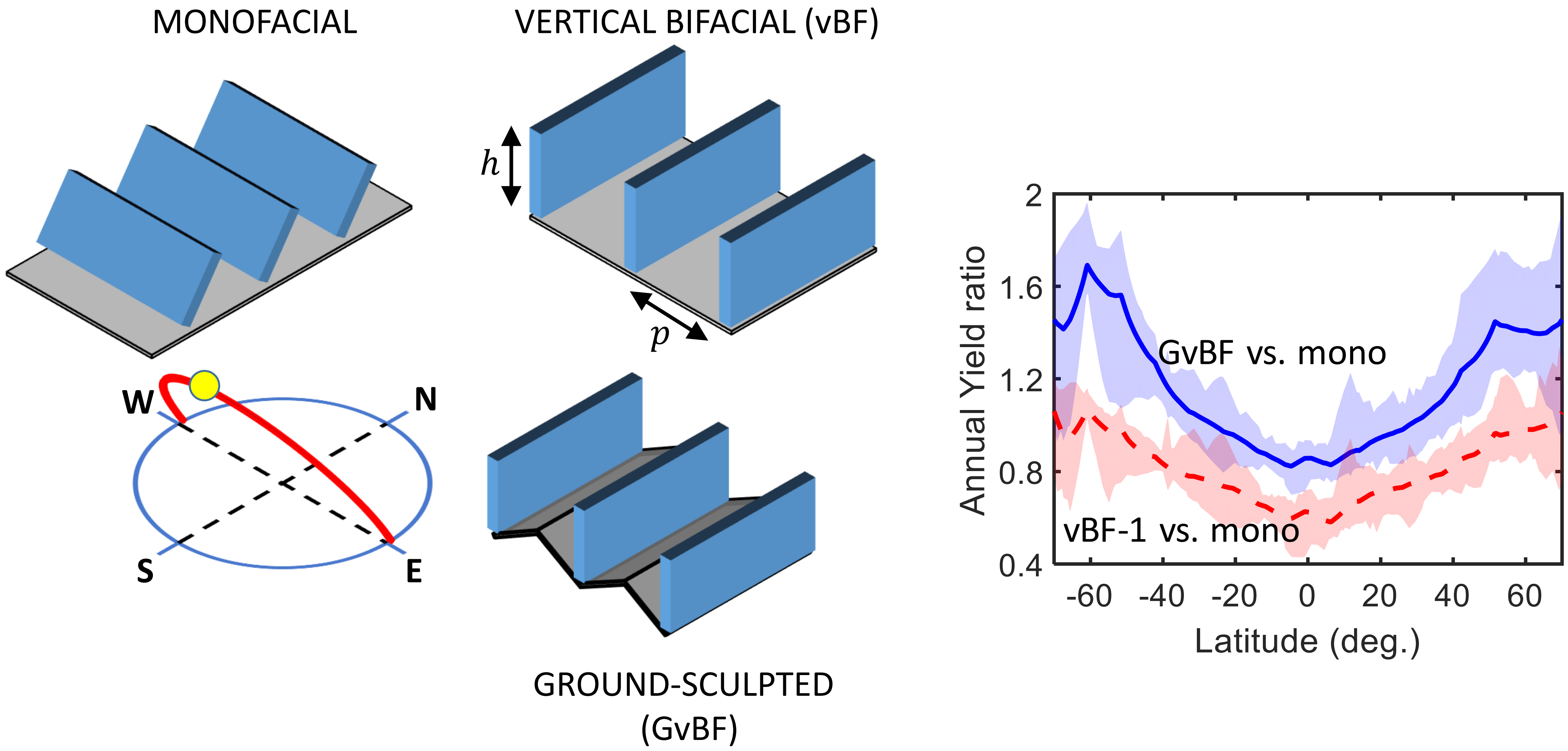
MONOFACIAL
VERTICAL BIFACIAL (vBF)
h
p
W
N
S
E
GROUND-SCULPTED
(GvBF)
Annual Yield ratio
2
1.6
1.2
0.8
0.4
-60
-40
-20
0
20
40
60
Latitude (deg.)
GvBF vs. mono
vBF-1 vs. mono